CHEMICAL ENGINEERING TRANSACTIONS
VOL. 86, 2021
A publication of AIDIC
The Italian Association of Chemical Engineering
Online at www.cetjournal.it
Guest Editors: Sauro Pierucci, Jiří Jaromír Klemeš
Copyright © 2021, AIDIC Servizi S.r.l.
ISBN 978-88-95608-84-6; **ISSN** 2283-9216

Galvanic Deposition Of Hydroxyapatite/Chitosan/Collagen Coatings On 304 Stainless Steel

Claudio Zanca[a,*], Germana Cordaro[a], Elisa Capuana[a], Valerio Brucato[a], Francesco Carfì Pavia[a], Vincenzo La Carrubba[a], Giulio Ghersi[b], Rosalinda Inguanta[a]

[a] Department of Engineering, University of Palermo, Viale delle Scienze - 90128 Palermo (Italy)
[b] Department of Biological, Chemical and Pharmaceutical Sciences and Technologies, Viale delle Scienze - 90128 Palermo (Italy)
claudio.zanca@unipa.it

The galvanic deposition method was used to deposit Hydroxyapatite/Chitosan/Collagen coatings on 304 stainless steel. Galvanic deposition is an alternative and valid way to fabricate bio-coatings with high biocompatibility and good anticorrosion properties. Physical-chemical characterizations were carried out to investigate chemical composition and morphology of the samples. Coatings consist of a mixture of calcium phosphate (Brushite and Hydroxyapatite) with chitosan and collagen. Corrosion tests were performed in the simulated body fluid (SBF) after different aging times. Results show that, in comparison with bare 304 stainless steel, coating shifts corrosion potential to anodic values and reduces corrosion current density. Nevertheless, the aging in SBF led to a completely conversion of brushite into hydroxyapatite. The release of metal ions, measured after 21 days of aging in SBF solution, is very low due to the presence of coating that slow-down the corrosion rate of steel.

1. Introduction

Over the last years, the use of metallic orthopedic implants for the treatment of different orthopedic traumas is constantly increasing because of the increase in the average life of patients. The most used materials are titanium and cobalt alloys and stainless steels thanks to their excellent mechanical properties close to human bones. Unfortunately, these materials in the body fluids can be subjected to corrosion phenomena that should not be underestimated, because led to the release of corrosion products around periprosthetic tissues. The release of metal ions could provoke allergenic and cancerogenic effects or a local destruction of soft and hard tissues, termed metallosis (Eliaz 2019). The worst cases could lead to unexpected breakdown of orthopedic implants to the detriment of patients. To overcome these mistakes, the research is focused on the use of coatings that act not only for protection against corrosion but also to overcome the bio-inertia of metals with bone tissue. In consequence, biocoatings must be composed of high biocompatible materials to decrease as much as possible the risk of rejection. Hydroxyapatite (HA), $Ca_{10}(PO_4)_6(OH)_2$, is a calcium phosphate compound that is the principal inorganic component of human bone that is made of nanocrystal of HA immersed in the matrix of collagen. Considering the human bone structure, different biopolymers (such as gelatin, chitin, chitosan and polylactic acid) have increasingly used with hydroxyapatite to increase the biocompatibility and bioactivity of biocoatings (Escobar-Sierra et al. 2015). In this work, hydroxyapatite/chitosan/collagen (HA/CS/CL) composite coatings were obtained via galvanic deposition method. This deposition method is a valid alternative for coatings fabrication respect to traditional ones (Harun et al. 2018). The main advantage is that no external power supply is required, nor special equipment or specialized personnel. As matter of fact, galvanic deposition method is based on a spontaneous redox reaction thanks to galvanic coupling between two metals characterized by different electrochemical redox potentials. Cathodic deposition reactions on the substrate (AISI 304) occur thanks to electrons generated by corrosion of zinc sheet that acts as sacrificial anode. Temperature and ratio of cathodic and anodic areas are the parameters used to control rate deposition of this process.

Physical-chemical characterizations were carried out on samples in order to evaluate chemical composition and morphology of the coatings. Corrosion tests were performed in simulated body fluid (SBF) to evaluate anticorrosion performances during 21 days of aging. Besides, cytotoxicity tests were carried out to attest biocompatibility of coatings.

2. Experimental

2.1 Galvanic deposition technique

Commercial AISI 304 stainless steel (SS) (bars of 70x15x3 mm) was utilized as substrate, while metal zinc (sheets of 70x30x2 mm) was selected as sacrificial anode for its low standard electrode potential (-0.76 V/NHE). SS substrates were degreased in ultrasonic bath with pure acetone for 5 minutes, mechanically polished with abrasive papers (from P150 to P1200 grade) and finally, rinsed ultrasonically in distilled water and acetone for two times, each lasting 5 minutes. After cleaning, SS surface was delimited with an insulating lacquer to expose an area of about 1.14 cm^2. The same treatment was used to pre-treatment the zinc sacrificial anode, and its exposed area was about 27 cm^2. SS was immersed in a solution of $Ca(NO_3)_2 \cdot 4 \cdot H2O$ (0.061 M), $NH_4H_2PO_4$ (0.036 M) and $NaNO_3$ (0.1 M), chitosan (CS) (5 gL^{-1}) and 0.3 mL acid lactic. Collagen (CL) was added to the solution at different concentration. The sacrificial anode was immersed in 40 mL of NaCl (1 M) and connected to the deposition solution (where SS was immersed) using agar/agar saturated KCl salt bridge. A freshly solution for each experiment was used, and the deposition process was carried out at 50°C for 24 h. After deposition, samples were dried in air.

2.2 Physical-chemical and electrochemical characterization

Coating morphology was examined by a QUANTA 200 FEI field emission gun (FEG) environmental Scanning Electron Microscope (SEM), and X-ray energy dispersive spectroscopy (EDS) was used to investigate chemical composition. Raman spectroscopy was performed by a Renishaw (inVia Raman Microscope) spectrometer equipped with He:Ne 532 nm laser. Analyses were carried out with 100% of laser power and a spot of 2 μm in different points of samples, performing three acquisitions for each analyzed point in the range between 3500 and 100 cm^{-1}. Raman peaks were identified by comparison with RHUFF database (Downs and Hall-Wallace, 2003). The coating crystallographic structure was investigated by X-ray diffraction using a RIGAKU diffractometer (model: D-MAX 25600 HK). All diffraction spectra were obtained in the 2θ range from 10° to 60° with a step of 0.004° and a measuring time of 0.1 sec for step, using the copper Kα radiation (λ= 1.54 Å). Diffraction patterns were analyzed by comparison with ICDD database.
Electrochemical characterizations were performed during 21 days of aging in Simulated Body Fluid (SBF) at 37°C. The preparation of SBF has been reported by Oyane et al. (2003). A conventional three-electrode cell, whit Pt wire and 3 M Ag/AgCl as counter and reference respectively, was used. Potentiodynamic Polarization (PP) and Electrochemical Impedance Spectroscopy (EIS) were executed. Corrosion potential (E_{corr}) and corrosion current density (i_{corr}) were evaluated by extrapolation of Tafel curves. EIS was performed in a frequencies range between 0.1 Hz and 100 kHz, with a 0.010 V of AC perturbation. Impedance data were processed using ZSimpWin software.

3. Results and discussion

3.1 Mechanism of deposition

To deposit HA/CS/CL coating on metallic substrate, galvanic deposition was used that takes advantage by galvanic coupling between stainless steel and zinc, characterized by a different electrochemical redox potential. The process was conducted in a separate cells system (Figure 1) where ionic conduction was ensured by saturate KCl salt bridge. Reactions on both electrodes start as soon as they were short-circuited and soaked in their own solutions. In the anodic compartment the reaction of zinc occurs as follow (1)

$$Zn \rightarrow Zn^{2+} + 2e^- \qquad (E° = -0.76 \text{ V/NHE}) \qquad (1)$$

Electrons produced by this reaction move towards cathodic compartment, where at working electrode surface the OH^- are produced by electrogeneration of base according to the following reactions (2-4)

$$NO_3^- + H_2O + 2e^- \rightarrow NO_2^- + 2OH^- \qquad (E^{eq} = 0.0835 - 0.059 \text{ pH V/NHE}) \qquad (2)$$

$$2H_2O + 2e^- \rightarrow 2OH^- + H_2 \qquad (E^{eq} = 0.0 - 0.059 \text{ pH V/NHE}) \qquad (3)$$

$O_2 + 2H_2O + 4e^- \rightarrow 4OH^-$ ($E^{eq} = 1.23 - 0.059$ pH V/NHE) (4)

The increasing of pH at cathode/electrolyte interface leads to the precipitation of calcium phosphate compounds with the mechanism reported in the previous works (Blanda et al. 2016). The production of OH^- ions increases the pH value of cathodic solution from 3.5 to 4.3. The increase of pH drives several equilibria reactions involving Ca^{2+} and $HPO4^{2-}$ leading the formation of BS and HA onto the metallic substrate. Furthermore, hydroxyl ions also cause the deprotonation of chitosan amine groups (reaction (5)) as reported in (Pang and Zhitomirsky 2007).

$Chit\text{-}NH_3^+ + OH^- \rightarrow Chit\text{-}NH_2 + H_2O$ (pKa= 6.4) (5)

The increase of interfacial pH is essential also for the deposition of the collagen fibrils that starts when the isoelectric point of this protein was reached (pH 7.4) (Zhuang et al. 2016). In particular, the collagen molecules charged positively close to cathode surface (SS substrate) were self-assembled and deposited. Thereby, co-deposition of biopolymers and calcium phosphate compounds occurs by the simple galvanic method.

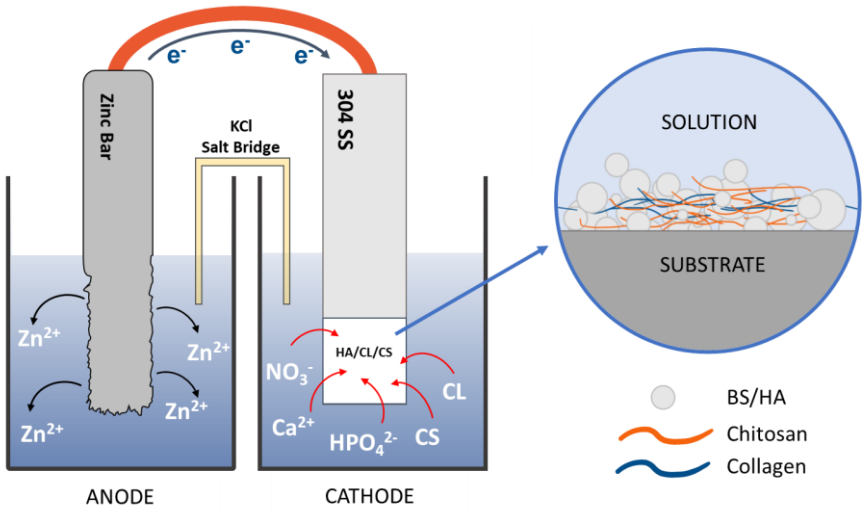

Figure 1: Separate cells system for galvanic deposition process

3.2 Physical chemical characterizations

In Figure 2a diffraction patterns of HA/CS and HA/CS/CL composite coatings were reported. HA and Brushite (BS) diffraction peaks were identified according to ICDD database (HA card n. 72-1243, BS card n. 72-0713). According to previous works (Mendolia et al. 2021), the increasing of local pH at the surface causes firstly BS formation and after the HA deposition. Thus, BS is the main phase while the presence of the polymers were not detected by this characterization method because have an amorphous nature and are present in low quantity. Furthermore, Raman Spectroscopy was executed in order investigate composition of the samples. Typical vibrational modes of HA and BS in Figure 2b are present and the results are coherent with XRD results. The fluorescence interference presents in the Raman spectrum can be attributable to the presence of polymers (Purcell and Bello, 1990).
EDS analyses were also performed to investigate the chemical composition of composite coatings. In Table 1 measured Ca/P values are reported. In particular, these measures are mean values obtained performing the analysis in different area of the coating. This ratio must be 1 and 1.667, for stoichiometric BS and HA, respectively, and measured ratios are comprised in this range. Thus, it is clear that the composite coatings are constituted by a mixture of BS and HA. As regards coatings containing collagen, it was observed that Ca/P value increases with CL dissolved in the cathodic solution. This result is coherent with XRD analyses, showing the HA peaks more intense than BS peaks in the HA/CS/CL sample rather than HA/CS ones. A qualitative information comes from Ca/Fe ratio, too. In particular, the higher value of Ca/Fe corresponds to a thicker coating. Thus, the presence of CL in solution is able to modify both composition and thickness of coatings.

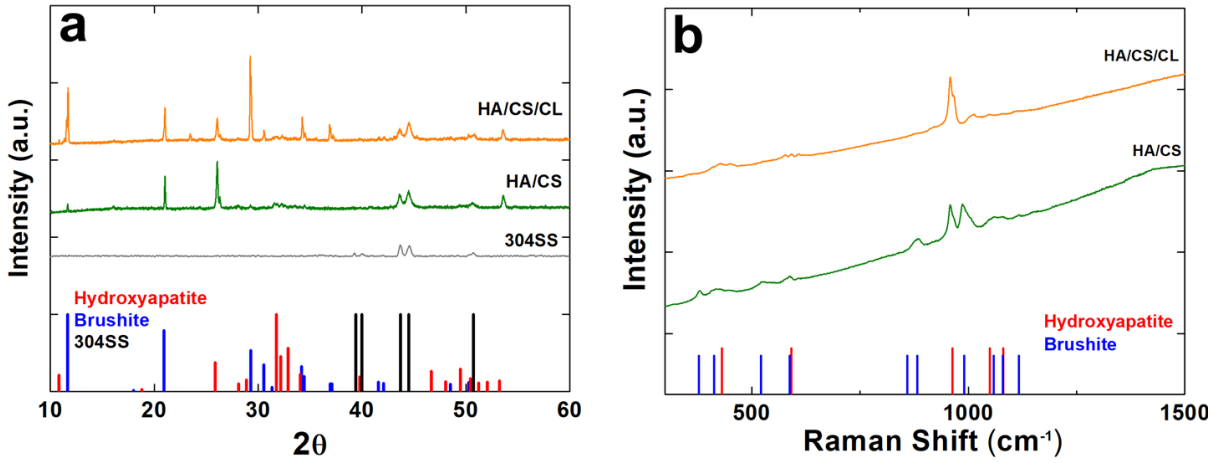

Figure 2: a) XRD patterns of HA/CS and HA/CS/CL obtained after 24 h at 50°C. b) Raman spectra of HA/CS and HA/CS/CL obtained after 24 h at 50°C.

SEM images show coating morphology reported in Figure 3. Coatings fabrication through galvanic deposition is able to cover the entire metallic surface of SS304. In Figure 3a the typical morphology of BS/HA coatings (without polymers) is shown. The presence of biopolymers in the coatings, Figure 3b (HA/CS) and Figure 3c (HA/CS/CL), greatly modifies the morphology of the samples. The round shapes are typical of CS morphology and are formed after the deposition during the drying in air due to the CS dehydration. At first glance the holes may seem empty, but inside a compact layer was found. Thus, the SS surface is completely covered also in these samples.

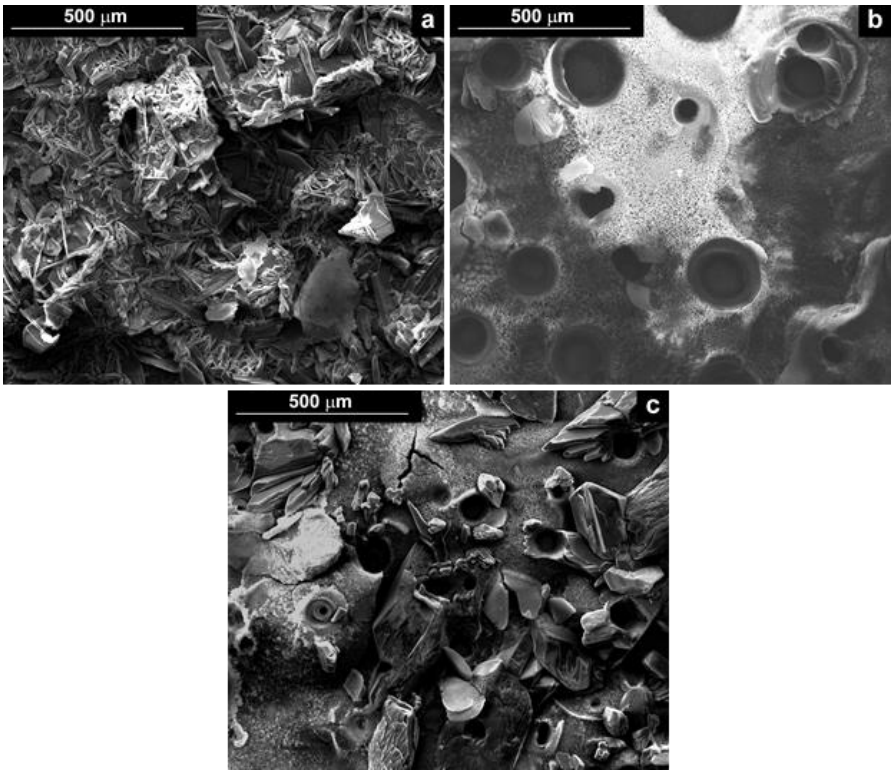

Figure 3: SEM images of composite coating of hydroxyapatite/chitosan/collagen at different concentration of collagen. a) HA/BS b) HA/CS c) HA/CS/CL

Table 1: Ca/P and Ca/Fe values of HA/CS/CL coating after 24 h of galvanic deposition at 50°C.

	Ca/P	Ca/Fe
HA/CS	1.29	11.72
HA/CS/CL	1.42	26.044

Physical-chemical characterizations of coatings were also performed after 21 days of aging in SBF solution to evaluate their stability. XRD diffraction reveals the absence of BS peaks after aging. These results are due to the reaction that involve BS and HA. In fact, according to Nur (2014), a BS/HA equilibrium (6) takes place at the interface following the reaction

$$10CaHPO_4 + 2OH^- \leftrightarrow Ca_{10}(PO_4)_6(OH)_2 + 4PO_4^{3-} + 10H^+ \quad (6)$$

3.3 Anticorrosion performances and cytotoxicity behavior

Anticorrosion performances were evaluated in vitro in SBF solution for 21 days at 37°C. Corrosion potential (E_{corr}) and corrosion current density (i_{corr}) were calculated by extrapolation of Tafel's curves shown in Figure 4. It was observed that during 21 days of aging, corrosion potential moves towards higher potential. The increase of E_{corr} is due to the coating protective action that acts as a physical barrier between SS substrate and SBF solution. As regards i_{corr}, calculated values are below respect to uncoated SS304, showing the decrease of corrosion rate phenomena. In Table 2 the corrosion potential (E_{corr}) and corrosion current density (i_{corr}) values at 21st day of aging for the different samples were reported.

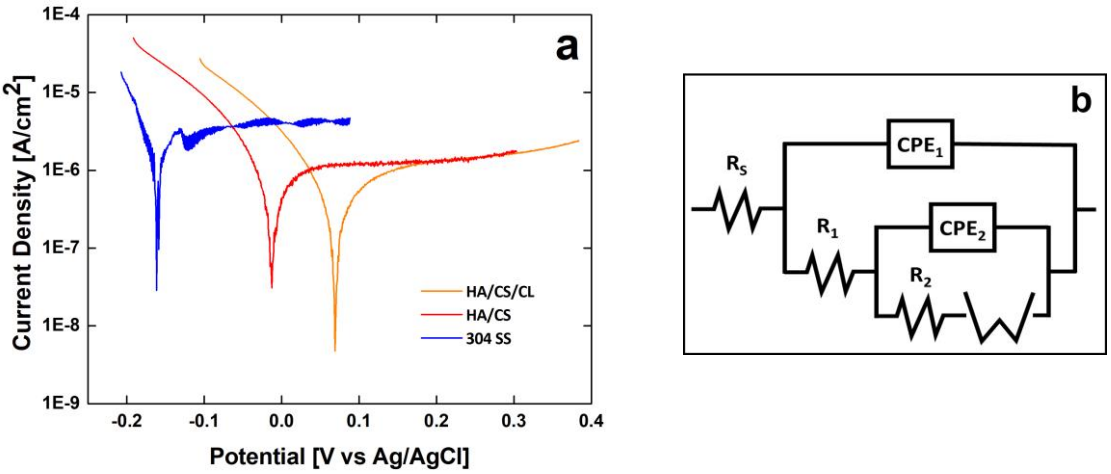

Figure 4: a) Tafel plots measured in SBF solution for HA/CS and HA/CS/CL coated samples obtained by galvanic deposition. For comparison, the plot relative to uncoated 304SS is also reported. b) Equivalent circuit used for impedance fitting

Table 2: Corrosion parameters of HA/CS and HA/CS/CL composite coatings. Bare 304 SS corrosion parameters were reported for comparison.

	E_{corr} [V]	I_{corr} [Acm^{-2}]
Bare 304SS	-0.161	3.92E-06
HA/CS	-0.017	8.51E-07
HA/CS/CL	0.071	8.22E-07

Impedance spectra were fitted by the equivalent circuit $R_s(CPE_1(R_1(CPE_2(R_2W))))$. R_s is related to the solution resistance, CPE_1 and R_1 simulate behaviour of outer porous layer of the coating and finally CPE_2 and R_2 simulate the behaviour of the film attached to metallic substrate. Warburg element was introduced to simulate diffusion process due to the dissolution/precipitation phenomena between BS and HA. The relative errors were less than 10% with a chi-square almost of 10^{-4}. These results show that the total impedance of coated sample is higher than un-coated SS. According the above results, this is due the protective action of coatings.

Metal ions released in SBF after aging was also quantified by ICP-OES. The metal release from uncoated 304SS was also analyzed, in order to compare the result with those relative to coated samples. Low ppm of Fe Ni and Cr ions were measured (below 0.05 ppm), coming from the corrosion of the metallic substrate. These values result below harmful concentration for human body (5 ppm Fe, 2 ppm Cr, 0.5 ppm Ni) (Leikin and Paloucek, 2008). This analysis is a further confirm the protective action of the coatings for the substrate. By ICP-OES also the concentration of Ca and P in the SBF before and after aging were measured. It was observed a different concentration of Ca and P ions at the end of 21st day of aging respect to freshly prepared SBF solution. This result is attributable to the equilibrium reaction between BS and HA during soaking in SBF, according Nur et al. (2014). Furthermore, results from cytotoxicity tests confirm that pre-osteoblasts' growth is not inhibited as an indication of non-cytotoxic behavior of coatings.

4. Conclusion

In this work, HA/CS/CL were obtained on 304 SS by means of galvanic deposition technique. Coatings are able to completely cover metallic substrate. Chemical composition and phases of the sample were investigated by EDS, XRD and RAMAN analyses that reveals a mixture of calcium phosphates (HA/BS). Electrochemical tests revel good corrosion performances given by the increasing corrosion potential and the decreasing corrosion current density. Fe Ni Cr ions concentrations in SBF after aging are below dangerous thresholds for human body. Cytotoxicity tests showed a high biocompatibility of HA/CS/CL composite coating that makes biocompatible SS304 surface. Thus, galvanic deposition is a viable and low-cost way to obtain biocompatible and anticorrosive coating respect to traditional deposition methods.

References

Blanda G., Brucato V., Carfì Pavia F., Greco S., Piazza S., Sunseri C., Inguanta R., 2016, Galvanic deposition and characterization of brushite/hydroxyapatite coatings on 316L stainless steel. Materials Science and Engineering: C, 64, 93-101.

Downs R.T. and Hall-Wallace M., 2003, The American Mineralogist Crystal Structure Database, American Mineralogist 88, 247-250.

Eliaz N., 2019, Corrosion of Metallic Biomaterials: A Review, Materials. 12, 407.

Escobar-Sierra D. M., Martins J., Ossa-Orozco C. P., 2015, Chitosan/hydroxyapatite scaffolds for tissue engineering manufacturing method effect comparison. Revista Facultad de Ingeniería Universidad de Antioquia, 75, 24-35.

Harun W. S. W., Asri R. I. M., Alias J., Zulkifli F. H., Kadirgama K., Ghani S. A. C., Shariffuddin J. H. M., 2018, A comprehensive review of hydroxyapatite-based coatings adhesion on metallic biomaterials. Ceramics International, 44(2), 1250-1268.

International Centre for Diffraction Data, 2007, Newtown Square, PA, U.S.A.

Leikin J.B., Paloucek F.P. (2008), Poisoning and toxicology handbook, 4th ed., Informa Healthcare

Mendolia I., Zanca C., Ganci F., Conoscenti G., Carfì Pavia F., Brucato V., La Carrubba V., Lopresti F., Piazza S., Sunseri C., Inguanta R., 2021, Calcium phosphate/polyvinyl acetate coatings on SS304 via galvanic co-deposition for orthopedic implant applications, Surface & Coating Technology, 408, 126771.

Nur A., Setyawan H., Widjaja A., Lenggoro I. W., 2014, Electrochemical processes for the formation of hydroxyapatite powders. Bulletin of Chemical Reaction Engineering & Catalysis, 9(3), 168.

Oyane A., Kim H. M., Furuya T., Kokubo T., Miyazaki T., Nakamura T., 2003, Preparation and assessment of revised simulated body fluids. Journal of Biomedical Materials Research Part A: An Official Journal of The Society for Biomaterials, The Japanese Society for Biomaterials, and The Australian Society for Biomaterials and the Korean Society for Biomaterials, 65(2), 188-195.

Pang X., Zhitomirsky I., 2007, Electrophoretic deposition of composite hydroxyapatite-chitosan coatings. Materials Characterization, 58(4), 339-348.

Purcell F. J., Bello J. M, 1990, Fluorescence-free Raman spectra of polymers, Raman and Luminescence Spectroscopies in Technology II (Vol. 1336, pp. 135-143).

Zhuang J., Lin J., Li J., Wang H., Cheng K., Weng W., 2016, Electrochemical deposition of mineralized BSA/collagen coating. Materials Science and Engineering: C, 66, 66-76.